# On the importance of atom probe tomography for the development of new nanoscale devices

Thales Borrely
Institute of Physics
University of São Paulo
São Paulo, Brazil
thales.santos@usp.br

Rachel S. Goldman

Material Science and Engineering

University of Michigan

Ann Arbor, United States

rsgold@umich.edu

Tao-Yu Huang

Material Science and Engineering
University of Michigan
Ann Arbor, United States
taoyuhu@umich.edu

Alain A. Quivy
Institute of Physics
University of São Paulo
São Paulo, Brazil
aquivy@if.usp.br

Yu-Chen Yang
Material Science and Engineering
University of Michigan
Ann Arbor, United States
yuchyang@umich.edu

Abstract—Atom probe tomography is the only technique capable of measuring with sub-nanometer resolution threedimensional spatial distributions of all chemical elements with no restrictions of mass or atomic number. The technique has been playing an important role in the development of all sorts of semiconductor devices. However, it is still somewhat littleknown outside of the most developed parts of the world. Bearing this in mind, this work aims to present and discuss the atom probe tomography technique and, more importantly, its impact on the development of nanoscale devices to the Brazilian Microelectronics Society. First, we introduce the working principles and experimental procedures of atom probe tomography. Next, we present a few real examples of applications of the technique to device development. Lastly, we briefly discuss the possibility of an application that has not been done yet, namely the atom probe tomography of submonolayer quantum dots.

Keywords—atom probe tomography, semiconductors, devices, chemical characterization, nanostructures

## I. INTRODUCTION

Atom probe tomography (APT) is a relatively new nanoscale characterization technique with features that no other technique has. APT combines field ion microscopy (FIM) and time-of-flight mass spectrometry (ToF-MS) to provide a three-dimensional (3D) spatial distribution of all elements with sub-nanometer resolution [1]. This unique capability of spatial-chemical characterization makes it a highly effective tool not only for materials science but also for other fields like geosciences and biology. The 3D compositional maps obtained by APT allow a deeper understanding of the optical and electronic properties of materials as well as their formation processes. As a result, APT can aid in the development of new materials, device design, and prediction of the long-term performance of devices. The information provided by the technique is also conveniently suitable for establishing ab initio simulation inputs.

It has been reported that 100 groups were equipped with APT systems worldwide in 2020 [2], a remarkably small number compared to other well-established characterization techniques such as x-ray diffractometry or scanning probe microscopy. This is not only due to APT being relatively new, but also because it is costly, as it requires two sophisticated ultra-high vacuum (UHV) systems: one for sample preparation and another one for the experiment. Naturally, this leads to APT being even rarer outside wealthier countries, e.g., in Latin America. Bearing this in mind, our present objective is to bring the relevance of APT to the attention of the

This study was financed in part by the Coordenação de Aperfeiçoamento de Pessoal de Nível Superior – Brasil (CAPES) – Finance Code 001

Brazilian Microelectronics Society by presenting the current and expected future impacts of this technique on materialsrelated research and development. Especial attention will be given to nanotechnological devices.

### II. WORKING PRINCIPLE

The path of least resistance for understanding APT is to comprehend the two techniques that originated it: FIM and ToF-MS. In FIM, a sharp cone-shaped metal specimen is placed in an UHV environment and submitted to high voltage, creating a strong electric field around the sample [3]. If intense enough, the voltage causes field ionization, i.e., it ionizes atoms that are around and close to the sample surface. If voltage is further increased, at some point it will provide surface atoms with enough energy to overcome their chemical bonds, causing them to detach from the sample—a phenomenon known as field evaporation. Once released from the surface, atoms start a nearly radial motion, and their trajectories are essentially governed by electrostatic [4]. They are then detected by an ion detector placed in front of the specimen (Fig. 1). The smaller the tip radius, the larger the ion trajectory divergence, which magnifies the tip typically in the order of 106, meaning that the resolution is in the order of magnitude of interatomic distances.

Time-of-flight mass spectrometry is a technique for obtaining the mass-to-charge ratio of ions by submitting them to a voltage while measuring the time they take to reach the detector (time-of-flight). The electric potential energy of a point charge depends only on its charge value. By equating the electric potential energy to the classical kinetic energy, one can easily conclude that the velocity of detected ions depends on their mass-to-charge ratio. The distance traveled by the ions to reach the detector is, of course, a known experimental parameter. Thus, measuring the time of flight gives us the velocity and, consequently, the mass-to-charge ratio [5].

In short, the APT technique consists in doing a FIM experiment while using ToF-MS to characterize the particles being ripped out of the specimen. The system needs to be equipped with a position-sensitive 2D detector so the original position of each particle in the specimen can be reconstructed from the position at which the particle is detected [2].

# III. EXPERIMENT AND ANALYSIS

The APT experiment starts with specimen preparation. This procedure takes place in a dual-beam scanning electron microscope/focused ion beam (SEM/FIB) system. SEM serves the purpose of monitoring the tip formation process and

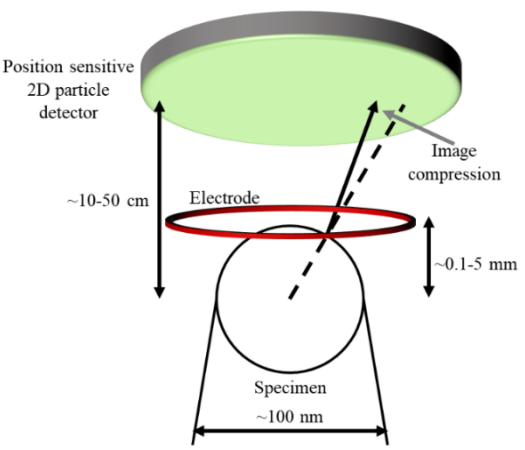


Fig. 1: Schematics of the APT experimental setup with indication of typical distances and dimensions. The deviation of ion trajectories from the radial direction that causes image compression is illustrated.

selecting the area where the tip will to be shaped, whereas FIB is used to make the tip. The standard procedure to shape the tip is the following (Fig. 2) [6]: (1) a ~5-15  $\mu m$ -long piece is cut out of the bulk with the FIB; (2) using a gas injection system, a micromanipulator is welded to that piece so it can be transferred to a support; (3) the piece is attached to the support and cut again with the FIB so only a small portion of the initial piece will remain on the support; (4) a series of ringshaped millings with different radiuses are done to shape the small piece on the support into a cone. Steps (3) and (4) can be repeated to make three or four specimens out of the initial ~15  $\mu m$ -long piece. The cone base has a typical radius of ~100 nm.

Once the specimen is ready, it can be transferred to the experimental station where the tip is evaporated using a high voltage or laser pulses, and the evaporated ions are collected. The raw data obtained from the experiment is a set of 3 coordinate points, namely the x and y spatial coordinates corresponding to the position at which the ions are detected by the 2D detector and their time of flight. The data analysis starts with the identification of ions on the mass-to-charge spectrum. Each peak in the spectrum needs to be assigned to an atomic or molecular ionic species. In the cases where two ionic species have the same mass-to-ratio values, isotope peaks can be used to dissolve any ambiguity [7].

Next is the reconstruction of the specimen from the raw data, that is, the determination of what the real-space position of each atom in the specimen is prior to the field evaporation. This process is done in two steps. In the first one, which can be understood as a reverse-projection of the detected positions on the specimen surface, it is assumed that the ions fly in a field-free environment, as this leads to the trajectory being independent of voltage, ions mass, and ion charge [4]. A reverse-projection framework is convenient, as the 2D detection coordinates can be associated with the 3D original position of ions without the need of calculating each ion trajectory [8, 9]. The ion trajectory is initially quasi-radial, but it curves towards the center of the detector causing an image compression that the reconstruction procedure must correct for. This compression depends on the shape of the tip and, therefore, there needs to be an a priori description of the tip geometry for the reconstruction to take place. The specimen is usually assumed to be a truncated cone with a hemispherical cap throughout the experiment [9]. As the tip is evaporated, however, the top base radius of the cone is enlarged. Thus, the time evolution of the tip shape also needs to be estimated either by relating the applied voltage—which is slowly increased to keep the detection rate constant—to the tip radius or by assuming a relation between the total ion count and the portion of the tip that is evaporated [9].

The second step of the reconstruction process is to determine the depth of each atom. The main assumptions in this step are: (1) atoms are only evaporated from the hemispherical surface; (2) the surface slowly moves away from the detector at a rate that is proportional to the volume occupied by the atoms in the specimen's lattice [9], which justifies why the analysis needs to start with the identification of the mass-to-charge ratio peaks.

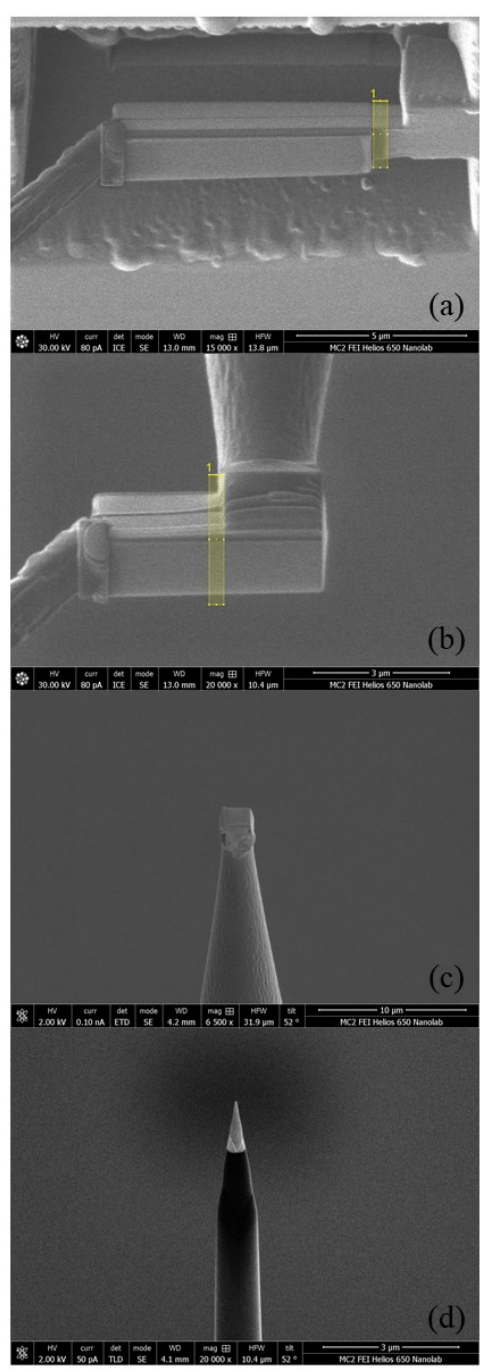


Fig. 2: SEM images of the sample-preparation steps. The yellow color represents the area where the FIB is going to cut next. (a) A selected piece of the sample is attached to a micromanipulator (on the left) before being completely removed from the bulk. (b) The selected piece is attached to a support. (c) A small portion of the selected piece is left on the support. (d) Final shape of the specimen after a series of ring-shaped millings.

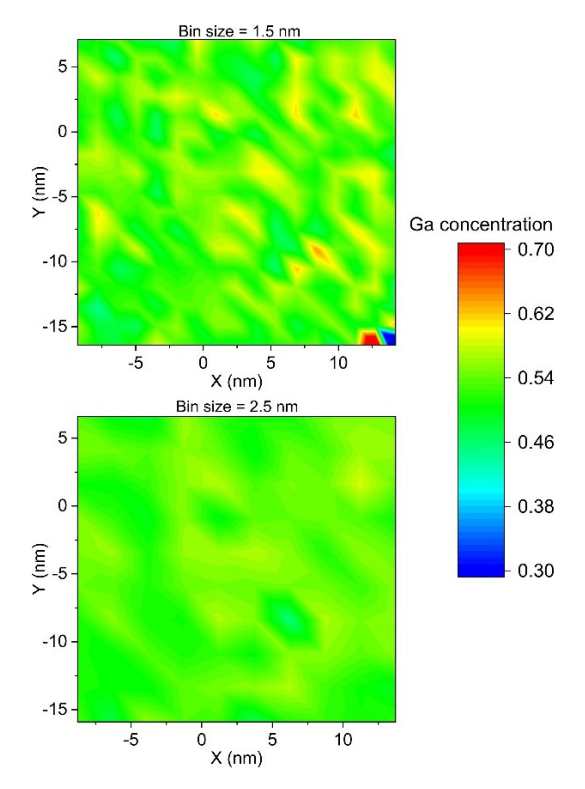


Fig. 3: Example of an APT result. Both figures are 2D contour plots representing the Ga percentage concentration in the same area of a GaAs sample grown by molecular beam epitaxy under standard conditions—i.e., a sample whose Ga content is certainly very close to 0.5. The only difference between the figures is the bin (voxel) size. With a bin = 1.5 nm (top), the Ga content varies tens of percentage points over the area, whereas a bin = 2.5 nm (bottom) leads to a fluctuation of only a few percentage points around 0.5. This means that 1.5 nm is below the spatial resolution limit and 2.5 nm is close to it. For the sake of comparison, FIB-based ToF secondary ions mass spectroscopy has a lateral spatial resolution in the order of tens of nanometers limited by the collision cascade resulting from the ion bombardment.

Generally, there are two method classes of data visualization one can use to interpret the APT results once the sample is fully reconstructed, namely interatomic distance methods and voxel methods. A typical example of the former is the nearest-neighbor analysis, which consists in comparing the distribution of distances between a solute atom and its nearest solute neighbors with the same distance distribution of an idealized system where the solute atoms are randomly distributed. The latter class consists in dividing the data set into subsets of same volume (typically in the order of nm<sup>3</sup>) or same number of atoms. These subsets are then grouped based on a density or composition criterion that is suitable for the analysis in question. The smallest possible size of voxels is limited by the experimental resolution (Fig. 3), which can be sub nanometric for metals and roughly a few nanometers for semiconductors. This difference is mainly due to the field screening of conductors being more efficient compared to non-conductors. As a result, the electrostatic field penetrates non-conductors deeper, causing not only surface atoms to be evaporated but also some of the atoms beneath them [10]. Laser-sample complex interactions that result from the comparable dimensions of wavelength and tip radius are also resolution-limiting factors [2].

## IV. APPLICATIONS

A major advantage of APT over other techniques is that it combines high spatial resolution with compositional characterization and 3D imaging of bulk features. This does not imply, of course, that it should substitute other techniques.

On the contrary, one can greatly benefit from applying it in combination with other characterization methods. One example of this is the study of epitaxial Al<sub>x</sub>In<sub>1-x</sub>P thin films grown at different temperatures [11]. High-angle annular dark-field scanning transmission electron microscopy (HAADF-STEM) characterization of such films showed only a ~5% variation of the local group-III fraction over the could analyzed volume that not account photoluminescence results. With APT, however, it became clear that phase separation was taking place in the samples, leading to compositional variations of up to 20% over distances of ~10 nm that are diluted over the typical volume analyzed in HAADF-STEM. The nanoscale compositional variation observed by APT was compatible with emission broadening and increase in carrier lifetime reported in photoluminescence measurements.

An interesting example of APT use for device research is the case of ZnO:Al/SiO<sub>2</sub>/Si Schottky diodes, which were studied with the purpose of understanding the Fermi-level pinning in oxide/Si interfaces, a topic that concerns the development of field-effect transistors and hot-carrier solar cells [12]. A change in the Schottky barrier height is expected as the free-electron concentration (n) in the ZnO:Al layer is varied from  $1\times10^{19}$  cm<sup>-3</sup> to  $8\times10^{20}$  cm<sup>-3</sup> due to the insulator-metal transition that takes place at n  $\approx 6\times10^{19}$  cm<sup>-3</sup>. However, the barrier height was shown to be nearly constant in the analyzed range. APT data showed a high concentration of Al within a distance of a few nanometers from the junction, causing the ZnO:Al film to be metallic close to the junction even when the bulk film was semiconducting.

APT has also been important for the development of quantum cascade lasers (QCL) [13]. AlInAs/GaInAs/InP QCLs grown by metal-organic chemical vapor deposition (MOCVD) have presented an unexpected 0.5-1.0 µm emission redshift relative to what was predicted by device design. Depth profiles obtained by APT indicated that the AlInAs/GaInAs interfaces are not as abrupt as commonly assumed in QCL modeling. On the contrary, the results showed that the compositional gradient at this interface is a few nanometers wide. In addition, there is an In accumulation at the AlInAs-to-GaInAs interfaces but not at the GaInAs-to-AlInAs interfaces. The addition of these structural features to the QCL models dissolved the incompatibility between theory and experiment and allowed the conclusion that non-abrupt interfaces do not compromise performance if they are taken into account in the device design.

A study on the spatial distribution of Si doping in epitaxial GaAs is a clear example of the advantages of APT over other mass-spectroscopy techniques such as time-of-flight secondary ion mass spectroscopy (ToF-SIMS) [14]. In that work, MOCVD was used to grow a few GaAs samples with different fluxes (φ) of Si precursor (Si<sub>2</sub>H<sub>6</sub>) ranging from 0.1 μmol/min to 225 μmol/min. As expected, ToF-SIMS showed that there is a monotonic increase of Si concentration from  $2 \times 10^{17}$  cm<sup>-3</sup> to  $6 \times 10^{20}$  cm<sup>-3</sup> as the Si precursor flux is respectively increased. Hall effect, however, indicated that the carrier concentration was in good agreement with the ToF-SIMS results only up to a Si concentration of 8×10<sup>18</sup> cm<sup>-3</sup> and a flux of 3  $\mu$ mol/min. For  $\varphi > 3 \mu$ mol/min, the Si concentration increased, but the carrier concentration decreased, indicating that Si does not act as a donor in GaAs once its concentration is above 8×10<sup>18</sup> cm<sup>-3</sup>. ToF-SIMS and Hall effect, however, do not provide any insights on what

happens to the Si atoms above this threshold value. APT imaging shows that the reason for the incompatibility between ToF-SIMS and Hall-effect results is not only a doping compensation phenomenon but also a nanoscale clustering of Si atoms above the threshold concentration. A first nearest neighbor analysis is used to confirm and quantify an increase in cluster concentration with increasing precursor flux. APT results like these are of remarkable importance, given how notoriously necessary doping is for microelectronic and photonic devices.

Lastly, we should mention a potential application of APT that has not been reported in the literature yet. One of the most studied nanostructures for device application is the quantum dot. Stranski-Krastanov quantum dots (SKQDs) are of particular interest for high-quality epitaxial semiconductor devices such as solar cells, lasers, infrared photodetectors, etc. SKQDs are nanocrystals that self-assemble during growth as a surface-energy minimization mechanism. This phenomenon takes place when material A is deposited on material B and the two materials have slightly different lattice constants (the difference is typically of a few percentage points). Despite being widely used, the SK method suffers from drawbacks that result from the self-assembling process such as lack of aspect-ratio control, low areal density, wetting layer formation, and creation of non-radiative recombination centers. Submonolayer quantum dots (SMLQDs) are being studied as potential substitutes for SKQDs. Simply put, SMLQDs are a vertical stack of small nanoscale islands of material A with a height of one monolayer (ML) that are spaced by a few MLs of material B. For growing SMLQDs, one needs to essentially: (1) Deposit less than 1 ML of material A to create a set of small islands; (2) Deposit a few MLs of material B; (3) Repeat steps (1) and (2) a few times. The vertical stack of islands is a natural consequence of the strain field caused by the difference between the lattice constants of materials A and B. In theory, the aspect ratio of SMLQDs can be tuned, as their height can be controlled by the number of cycle repetitions. Furthermore, SMLQDs do not rely on strain as much as SKQDs and, therefore, are expected to cause less crystalline defects. One of the challenges in SMLQD research is the chemical and morphological characterization of these structures, as they cannot be characterized by standard surface techniques such as atomic force microscopy because epitaxial thin spacer layers are a necessary part of SMLQDs-differently from SKQDs, which can be easily grown on a free epitaxial surface. In the case of In<sub>x</sub>Ga<sub>1-x</sub>As SMLQDs grown in a GaAs matrix [15], for instance, although cross-sectional scanning tunneling microscopy (XSTM) has been used in their study, precise chemical and morphological characterizations that allow a full understanding of the high-performance of SMLQD photoelectronic devices [16] have not yet been done. XSTM data showed that the dimensions of In<sub>x</sub>Ga<sub>1-x</sub>As SMLQDs are in the order of a few nanometers and part of the In is dissolved in the GaAs matrix. This was enough to support rough models that describe SMLQDs as perfect spheres in an In<sub>x</sub>Ga<sub>1-x</sub>As quantum well with low In content [17]. However, more with reliable simulations spatial-chemical distribution inputs have not been possible yet, and the workings of In<sub>x</sub>Ga<sub>1-x</sub>As SMLQD-based devices are still to be unveiled. APT is certainly the most suitable technique to provide reliable information on the distribution of these SMLQDs in the GaAs bulk, and to observe both the morphology and spatial distribution of the group-III elements.

## V. CONCLUSION

We have introduced the working principles and experimental procedure of atom probe tomography, a technique with unique spatial-chemical characterization capabilities. In addition, we have discussed examples of the use of APT for the development of materials and devices. By means of literature review, we have shown that APT is a suitable tool for understanding the growth dynamics of epitaxial and non-epitaxial thin films, including phenomena such as segregation, diffusion, and clustering, that lead to nanoscale compositional variations. Finally, we have briefly discussed a still unexplored potential of APT, namely the characterization of submonolayer quantum dots. The case of SMLQDs illustrates the fact that there are still many research programs on device development that could greatly benefit from unrealized potentials of APT.

#### REFERENCES

- [1] T. F. Kelly and D. J. Larson, "Atom Probe Tomography 2012", Annual Review of Materials Research, 2012, 42:1, pp. 1–31.
- [2] B. Gault, A. Chiaramonti, O. Cojocaru-Mirédin, et al., "Atom probe tomography", Nat. Rev. Methods Primers 1:51, pp. 1–30, 2021.
- [3] D. G. Brandon, "On field evaporation", The Philosophical Magazine: A Journal of Theoretical Experimental and Applied Physics, 14:130, pp. 803–820, 1966.
- [4] R. Smith and J. M. Walls, "Ion trajectories in field-ion microscope", J. Phys. D-Applied Phys, 11, pp. 409–419, 1978.
- [5] B. A. Mamyrin, "Time-of-flight mass spectrometry (concepts, achievements, and prospects)", International Journal of Mass Spectrometry, 206:3, pp. 251–266, 2001.
- [6] C. Greenhill, A. S. Chang, E. S. Zech, et al., "Influence of quantum dot morphology on the optical properties of GaSb/GaAs multilayers" Appl. Phys. Lett. 116, pp. 252107, 2020.
- [7] J. T. Sebastian, O. C. Hellman, and D. N. Seidman, "New method for the calibration of three-dimensional atom-probe mass spectra", Rev. Sci. Instrum., 72, pp. 2984–2988, 2001.
- [8] T. J. Wilkes, G. D. W. Smith, D. A. Smith, "On the quantitative analysis of field-ion micrographs", Metallography, 7:5, pp. 403–430, 1974.
- [9] P. Bas, A. Bostel, B. Deconihout, and D. Blavette, "A general protocol for the reconstruction of 3D atom probe data", Appl. Surf. Sci., 87–88, pp. 298–304, 1995.
- [10] T. T. Tsong, "Field penetration and band bending for semiconductor of simple geometries in high electric fields", Surf. Sci. 81, pp. 1–18, 1979.
- [11] K. Mukherjee, A. G. Norman, A. J. Akey, et al., "Spontaneous lateral phase separation of AlInP during thin film growth and its effect on luminescence", Journal of Applied Physics, 118, pp. 115306, 2015.
- [12] R. Jaramillo, A. Youssef, A. Akey, F. Schoofs, S. Ramanathan, and T. Buonassisi, "Using Atom-Probe Tomography to Understand ZnO:Al/SiO<sub>2</sub>/Si Schottky Diodes", Phys. Rev. Applied, 6, pp. 034016, 2016.
- [13] C. A. Wang, B. Schwarz, D. F. Siriani, et al., "Sensitivity of heterointerfaces on emission wavelength of quantum cascade lasers", Journal of Crystal Growth, 464, 15, pp. 215-220, 2017.
- [14] G. Beainy, R. Alcotte, F. Bassani, "Direct examination of Si atoms spatial distribution and clustering in GaAs thin films with atom probe tomography", Scripta Materialia, 153, pp. 109–113, 2018.
- [15] R. S. R. Gajjela, A. L. Hendriks, A. Alzeidan, et al., "Cross-sectional scanning tunneling microscopy of InAs/GaAs(001) submonolayer quantum dots", Phys. Rev. Materials, 4, pp. 114601, 2020.
- [16] A. Alzeidan, T.F. Cantalice, K.D. Vallejo, et al., "Effect of As flux on InAs submonolayer quantum dot formation for infrared photodetectors", Sensors and Actuators A: Physical, 334, pp. 113357, 2022.
- [17] S. Harrison, M. P. Young, P. D. Hodgson, et al, "Heterodimensional charge-carrier confinement in stacked submonolayer InAs in GaAs", Phys. Rev. B, 93, pp. 085302, 2016.